EXPERIMENTAL ANALYSIS ON THE INNER VORTICES INTERACTION ABOVE DIAMOND WING MODEL IN LOW SPEED AERODYNAMICS

MAZURIAH BINTI SAID

A thesis submitted in fulfilment of the
requirements for the award of the degree of
Doctor of Philosophy

School of Mechanical Engineering
Faculty of Engineering
Universiti Teknologi Malaysia

NOVEMBER 2021

DEDICATION

"Allah will raise those who have believed among you and those who were given knowledge, by degrees. And Allah is Acquainted with what you do."
[58:11]

Specially dedicated to the LOVE of my life

Always in my DOA and heart

Mak & Abah
Halimah Ahmad (1953 - 2000) & Said Taha (1936 - 2010)
Both whom the first to teach me to pursue and love knowledge.
I really miss both of you.
Al-Fatihah

My Family: Siblings, Nieces and Nephews
Those who always give their trust and support in whichever road I chose

Myself
MAZURIAH BINTI SAID

Be proud of yourself, you have striven for your innocent-self dream.

Allah has perfect timing; never early, never late. It takes a little patience and a lot of faith, but it's worth the wait.

ACKNOWLEDGEMENT

ALHAMDULILLAH praises to Allah. He who allowed and eased this journey for me to be able to finish this thesis. I take this opportunity to express my sincere appreciation to my supervisor Ir. Dr Shabudin Mat for giving me opportunity to work under his supervision. His supports, encouragements, guidance, motivations, critics and great welfare throughout the project has been invaluable. I am also thankful to my co-supervisors Dr Md Nizam Dahalan and Professor Ir. Dr Shuhaimi Mansor for their advices and support in the completing this study.

I also want to acknowledge the contribution of the UTM Aerolab technical staff in particular to Mr. Abdul Basid, Mr. Salahuddin, Mr. Mahathir and Mr. Akmal for their valuable times, helps and efforts who has been involved in the project to setup the model and their assistance during the experiments.

Very special thanks to my indispensable friend Mr. Airi Ali for helping me with the data acquisition programs for pressure measurements and contour mapping plots program. His guidance at various stages of work has been of immense help.

Life in the lab is not complete without having fellow postgraduate student and researchers to share your excitements and frustrations. My thanks to Amri for always ready to help for whatever help I need. My other fellow researchers and friends Mr Wan Zaidi, Amalina, Ernie, Izzwa, Farhanah, Ismah, Nadhirah, Faizira and others who have provided assistance at various occasions. Unfortunately, it is not possible to list all of them in this limited space. Thanks to you all for your friendship, help and support.

I am also indebted to Universiti Teknologi Malaysia (UTM) for funding my Ph.D study for four semester under Zamalah Scholarship. I would also to thank Ministry of Higher Education Malaysia (MOHE) for their financial support through the Research University Grant, RUG Tier 1 (Vot 18H06) and Fundamental Research Grant Scheme, FRGS (Vot. 4F718 & 21H05).

Last but not the least, my heartfelt thanks to my family for always being there for me. Thanks for your constant support through the ups and downs of my life. THANK YOU to each of everyone who involved in this project. Without you all, this work would not be happened.

ABSTRACT

Every country needs a high-speed Unmanned Air Vehicle (UAV) to monitor territory especially their ocean. One of the best UAV that can perform this mission is Unmanned Combat Air Vehicle (UCAV). The main advantage of the UCAV is a kind of delta-shaped drone that can fly at high speed and greater altitude. For a high-speed plane, there are always issues in the take-off and landing segments, as it need a longer runway. Thus, the aerodynamic performances at these conditions were always in transitional and not stable when it manoeuvres. North Atlantic Treaty Organisation (NATO) has initiated a task group of AVT-183 to perform the aerodynamic analysis on UCAV related profile recently. The flow above of Stability And Control CONfiguration (SACCON) wing is very complicated and a simplified model called Diamond wing was introduced for the aerodynamic studies. Diamond wing is also a kind of delta-shaped wing where at certain angle of attack, the primary vortex and other separation occur on the wing. The outcomes from the AVT-183 group were the flow on the upper surface of the Diamond flow field such as the vortical structures interaction, formation and progression are complicated, disorganised and unknown. Although many computer fluid dynamic researches have been conducted during the campaign, the data from the experiment or wind tunnel testing to validate the simulation is very limited especially in the inboard region. Thus, the numerical prediction of aerodynamic performance for the wing is not well predicted. The aim of this study was to provide the experimental data on the Diamond wing that can improve the understanding of the aerodynamic characteristics and the flow topology above the Diamond wing. This study assessed the formation, progression and interaction of vortices above the Diamond wing. A half-span NATO configuration Diamond-shaped wing model was designed and manufactured. The model was then tested in UTM – Aerolab subsonic wind tunnel at the Reynolds number of 1×10^6, 2×10^6 and 3×10^6, respectively. Four measurement techniques were employed on the wing, i.e., steady/unsteady force measurement, flow visualization, surface pressure measurement and finally the off-surface pressure study. The data obtained from the Diamond wing were compared with another delta-shaped NATO standard profile called VFE-2 wing. A model of VFE-2 wing was also fabricated in UTM, and several measurement techniques such as flow visualization and pressure measurements were performed on this wing. The main flow characteristics above the Diamond and VFE-2 wing were the primary vortex that occurred in the leading edge of the wing. The results from the tuft technique carried out in UTM has identified several relationships between the attached flow, primary and inner vortices. The results obtained have shown that lift and drag (L/D) ratio for the Diamond in the subsonic region has not been affected by the Reynolds number variation. The optimum lift is produced at angle of attack ranges between $3° < \alpha < 5°$ where the lift is 8 times higher than the drag. The lift for Diamond wing has increased by 9% when compared to the VFE-2 wing in the region where inner vortex was developed. However, the drag for the Diamond wing increased by up to 15% when compared to VFE-2 wing at the angle of attack 12° and above. The onset of the primary vortex for Diamond wing occurred at 20% chord-wise position earlier compared to VFE-2 wing. Interestingly, further inboard of the wing, several other vortices have been found. The number of vortices is depending on the flow conditions and these vortices have the same attributes as the inner vortex. This new discovery vortex is termed as *multi - inner vortex*. For the VFE-2 wing, there is only one single inner vortex developed inboard of the wing. It happened in the region 30% inboard of the wing span. The inner vortex has low intensity, which has about 85% pressure difference when compared to the corresponding primary vortex. This thesis provides a complete experimental data on flow above the Diamond wing. It also provided a better insight on the flow topology above the Diamond wing.

ABSTRAK

Setiap negara memerlukan sebuah kenderaan udara tanpa pemandu (UAV) pantas bagi tujuan kawalan sempadan terutamanya di kawasan perairan negara. UAV yang paling sesuai untuk tujuan ini adalah kenderaan udara tempur tanpa pemandu (UCAV). Kelebihan utama yang ada pada UCAV ini adalah dari sifat bentuk deltanya yang membolehkannya terbang pada kelajuan dan altitude tinggi. Bagi sesebuah pesawat pantas, masalah yang sering dihadapi adalah pada ketika ruas berlepas dan mendarat, kerana ianya memerlukan landasan yang cukup panjang. Oleh itu, prestasi aerodinamik pada keadaan tersebut berubah-ubah dan tidak stabil ketika olahgerak. Ini telah mendorong pihak Pertubuhan Perjanjian Atlantik Utara (NATO) untuk menubuhkan sebuah kumpulan dikenali sebagai AVT-183 bagi menjalankan analisis aerodinamik ke atas susuk sayap berkaitan. Aliran udara yang berlaku di atas sayap Konfigurasi Kestabilan Dan Kawalan (SACCON) sangat rumit, maka sebuah model sayap dipermudah dinamakan Berlian diperkenalkan bagi tujuan kajian aerodinamik ini. Sayap Berlian juga merupakan sejenis sayap berbentuk delta, yang mana pada sudut serang tertentu, vorteks utama dan lain-lain aliran terpisah berlaku di atasnya. Hasil kajian daripada kumpulan AVT-183 ini mendapati bahawa aliran udara pada permukaan atas Berlian seperti interaksi, pembentukan dan perkembangan struktur pusaran adalah rumit, tidak teratur dan tidak diketahui. Walaupun banyak penyelidikan komputasi dinamik bendalir telah dilakukan selama kempen berlangsung, data dari eksperimen atau pengujian terowong angin untuk pengesahan sangat terhad terutamanya pada kawasan dalam sayap. Hal ini menyebabkan ramalan berangka prestasi aerodinamik bagi sayap berkenaan tidak diramal dengan tepat. Tujuan penyelidikan ini dijalankan adalah untuk menyediakan data eksperimen sayap Berlian supaya pemahaman berkenaan topologi aliran dan ciri-ciri aerodinamik dapat ditingkatkan. Pembentukan, perkembangan dan interaksi pusaran di atas sayap Berlian telah diselidiki. Sebuah model sayap separuh rentang berbentuk berlian dan mengikut konfigurasi NATO direka dan dibina. Model in kemudiannya diuji di terowong angin subbunyi Aerolab – UTM pada setiap nombor Reynolds 1×10^6, 2×10^6 dan 3×10^6. Empat teknik pengukuran digunakan, iaitu pengukuran bebanan secara stabil/tidak stabil, gambaran aliran, pengukuran tekanan permukaan dan kajian tekanan di atas permukaan sayap. Data yang diperoleh daripada sayap Berlian dibandingkan dengan satu lagi susuk delta yang dirujuk sebagai model piawai oleh NATO iaitu sayap VFE-2. Sebuah model sayap VFE-2 juga dibina di UTM, dan beberapa teknik pengukuran seperti gambaran aliran dan pengukuran tekanan juga dilakukan ke atas sayap ini. Ciri utama yang terjadi di dalam aliran sayap Berlian dan VFE-2 adalah berlakunya vorteks utama di pinggir depan sayap. Hasil daripada teknik *tuft* yang dijalankan di UTM, beberapa hubungan di antara aliran melekat, vorteks utama dan vorteks dalam telah dikenalpasti. Keputusan eksperimen yang diperolehi menunjukkan bahawa nisbah daya angkat berbanding daya seret (L/D) bagi sayap Berlian tidak dipengaruhi oleh perubahan nombor Reynolds. Daya angkat yang optimum berlaku pada julat sudut serang $3° < \alpha < 5°$, yang mana daya angkat adalah 8 kali lebih tinggi daripada daya seret. Daya angkat untuk sayap Berlian meningkat sebanyak 9% jika dibandingkan dengan sayap VFE-2 untuk situasi yang mana vorteks dalaman terbentuk. Daya seretan untuk sayap Berlian meningkat sehingga 15% berbanding dengan sayap VFE-2 bermula pada sudut serang 12° dan ke atas. Titik mula vorteks utama berlaku pada kedudukan 20% mengikut-perentas lebih awal untuk sayap Berlian berbanding sayap VFE-2. Menariknya dalam kajian ini, beberapa lagi vorteks dalaman terbentuk di bahagian tengah sayap Berlian berbanding cuma satu sahaja vortex dalaman terbentuk untuk kes sayap VFE-2. Bilangan vorteks ini bergantung kepada keadaan aliran udara dan vorteks ini mempunyai sifat yang sama seperti vorteks dalaman. Penemuan vorteks baru ini diistilahkan sebagai vorteks dalam-berbilang. Ia terletak dalam lingkungan 30% di bahagian dalam sayap tersebut. Vorteks dalaman ini mempunyai keamatan yang rendah dengan mempunyai kira-kira 85% beza tekanan jika dibandingkan dengan vorteks utama. Tesis ini telah menyediakan data eksperimen yang lengkap mengenai aliran di atas sayap Berlian. Ianya juga dapat memberikan gambaran yang lebih baik mengenai topologi aliran di atas sayap Berlian.

TABLE OF CONTENTS

	TITLE	PAGE
	DECLARATION	**iii**
	DEDICATION	**iv**
	ACKNOWLEDGEMENT	**v**
	ABSTRACT	**vi**
	ABSTRAK	**vii**
	TABLE OF CONTENTS	**viii**
	LIST OF TABLES	**xii**
	LIST OF FIGURES	**xiii**
	LIST OF ABBREVIATIONS	**xix**
	LIST OF SYMBOLS	**xx**
	LIST OF APPENDICES	**xxi**
CHAPTER 1	**INTRODUCTION**	**1**
1.1	Introduction	1
1.2	Problem Statement	10
1.3	Research Objectives	12
1.4	Research Scope	12
1.5	Significance of the study	13
CHAPTER 2	**LITERATURE REVIEW**	**15**
2.1	Delta winged Unmanned Combat Air Vehicle	15
2.2	The Fundamental of the Vortex	17
	2.2.1 Leading-edge Vortex	18
2.3	The Influence of the Edge and Swept of the Wing to Aerodynamics	23
2.3	Slender: Blunt Delta Wing Flow Field	25
	2.3.1 The Region with Attached Flow	28
	2.3.2 The Region of Leading-Edge Separation	29

2.3.3 VFE-2 Inner Vortex Discovery 32
2.4 Non-Slender: Diamond Wing Flow Field 34
2.4.1 The Insipient Separation 35
2.4.2 Characteristics of Inner Vortex of Diamond Wing 36
2.5 Factors Influencing the Flow Field of Blunt-edge Diamond Wing 39
2.6 Numerical and Experimental Studies 42
2.7 Unresolved Issues on Blunt-edged Diamond Wing 55

CHAPTER 3 RESEARCH METHODOLOGY 57
3.1 Introduction 57
3.2 UTM-LST Wind Tunnel Facility 59
3.3 UTM VFE-2 wing model Descriptions 60
3.4 UTM Diamond Wing Model Descriptions 63
3.5 Wind Tunnel Testing 67
3.5.1 Wind Tunnel Testing of UTM VFE-2 Wing 67
3.5.2 Wind Tunnel Testing of UTM Diamond Wing 71
3.5.2.1 Steady and Unsteady Balance Measurements 73
3.5.3 Flow Visualization Testing 76
3.5.4 On – Surface Pressure Measurement 78
3.5.5 Off-surface Pressure Measurements 81
3.5.5.1 KULITE Miniature Dynamic Pressure Transducer Calibration 86
3.5.5.2 Limitation for the Off – Surface Pressure Measurement 88
3.6 Kriging Method 89

CHAPTER 4 RESULTS AND DISCUSSIONS – STEADY / UNSTEADY BALANCE 93
4.1 STEADY BALANCE MEASUREMENT 93
4.1.1 Introduction to Balance Measurements 93
4.1.2 Repeatability Test 94
4.2 The Aerodynamic Coefficients Analysis 97

4.2.1 Reynolds Number and Angle of Attack Effects on the Steady Forces 97

4.2.2 Reynolds Number and Angle of Attack Effects on Pitching Moment 101

4.2.3 Comparison of Diamond and VFE-2 Wings on Lift Coefficient 102

4.3 Summary of Steady Balance on Aerodynamic Coefficients Analysis 104

4.4 UNSTEADY BALANCE MEASUREMENT 106

4.4.1 Balance Compatibility Justification 106

4.4.2 Structural Vibration Natural Frequency Identification 107

4.4.3 Angle of Attack Effects on Unsteady Normal Forces 108

CHAPTER 5 RESULTS AND DISCUSSIONS – TUFT FLOW VISUALIZATION 113

5.1 Introduction 113

5.2 Observations at Reynolds Number of 1×10^6 (Re_{mac} = 0.66×10^6) 113

5.3 Observations at Reynolds Number of 2×10^6 (Re_{mac} = 1.3×10^6) 117

5.4 Observations at Reynolds Number of 3×10^6 (Re_{mac} = 2×10^6) 121

5.5 Comparison flow visualization of Diamond wing and VFE-2 wing. 124

5.6 Summary from Flow Visualization Studies 125

CHAPTER 6 RESULTS AND DISCUSSIONS – FLOW TOPOLOGY ANALYSIS 127

6.1 ON – SURFACE PRESSURES MEASUREMENT 127

6.1.1 Surface Pressure Verification with NATO experiments 127

6.2 Reynolds Number and Angle of Attack Effects 130

6.2.1 Surface Pressure Distributions 130

6.2.2 Leading edge Pressures Study 139

6.2.3 Surface Pressures Contour 146

6.3 Correlation of Surface Pressure Distributions and Aerodynamics Coefficient 152

6.4 OFF – SURFACE PRESSURES MEASUREMENT 154

6.4.1 Effects of Angle of Attack 154

6.4.2 Inboard Separation 163

6.4.3 Effects of Reynold number on vortex interaction 167

6.5 Summary of Flow Topology Analysis 173

CHAPTER 7 CONCLUSIONS AND RECOMMENDATIONS 175

7.1 Research Conclusions 175

7.2 Recommendations for Future Work 178

REFERENCES 181

LIST OF PUBLICATIONS 206

LIST OF TABLES

TABLE NO.	TITLE	PAGE
Table 2.1	NATO Facets on blunt-edged delta wing	26
Table 2.2	VFE-2 Delta wing experimental approached	48
Table 2.3	AVT-183 Diamond wing experimental approached	49
Table 2.5	Vortex predictive capability (Luckring, 2019)	56
Table 3.1	UTM-LST Flow Characteristics	59
Table 3.2	UTM VFE-2 delta wing profiles	61
Table 3.3	UTM Aerolab Diamond wing parameters	64
Table 3.4	Corresponding free stream velocity to Reynolds number and Re_{mac}	72
Table 3.5	JR3 Balance Load Range and Resolution	74
Table 3.6	Semi-span Balance Load Range	75

LIST OF FIGURES

FIGURE NO.	TITLE	PAGE
Figure 1.1	Slender vs. non-slender types of Delta wing	2
Figure 1.2	Types of Delta wing configurations (Pevitt and Alam, 2014)	3
Figure 1.3	Reynolds number range for UAV (Gursul, 2004)	3
Figure 1.4	Current and future UCAV design	4
Figure 1.5	Diamond shaped X-47A UCAV	5
Figure 1.6	The AVT-113 experimental model and testing in NASA wind tunnel (Luckring, 1996)	6
Figure 1.7	AVT-161 SACCON model and configurations (Cummings and Schütte, 2012)	7
Figure 1.8	Complex SACCON flow field (Fink, 2010; Cummings and Schütte, 2012)	8
Figure 1.9	NATO hierarchical decomposition of aerodynamic complexity connection to SACCON (Luckring et al., 2016)	8
Figure 1.10	AVT-183 Diamond wing configuration as simplified AVT-161 SACCON (Luckring et. al., 2016)	9
Figure 2.1	Diamond shaped UCAV / UAV (Ball, 2017; Airforce Technology, n.d.)	16
Figure 2.2	Vortex of conventional tapered wing (Ashifkhan, n.d.)	17
Figure 2.3	Pressure distributions on a delta wing (Anderson, 2001)	18
Figure 2.4	Formation of vortex on delta wing with sharp-edged (Pershing, 1964)	19
Figure 2.5	Surface suction of vortex induced-lift increments (Kulfan, 1979; Polhamus, 1966; Luckring, 2013)	20
Figure 2.6	General vortex structures on sharp-edge delta wing (Anderson, 1991)	21
Figure 2.7	The internal structure of primary vortex (Earnshaw, 1962)	22
Figure 2.8	Distribution of circumferential velocities of vortex (Earnshaw, 1962)	22

Figure 2.9	Concept of rounded leading-edge suction force (Rinoie, 1996)	23
Figure 2.10	Wing aspect ratio effects on the vortex-lift prediction (Polhamus, 1966)	25
Figure 2.11	Installation of VFE-2 wing in NASA Wind Tunnel (Luckring, 2013)	27
Figure 2.12	Summary of primary vortex separation of leading-edge bluntness effects (Luckring, 2004).	27
Figure 2.13	The surface pressure distributions of bluntness effects (Chu and Luckring, 1996)	28
Figure 2.14	Oil flow visualization experiment on large-edge wing at α = 13.3° for Re_{mac} = 1× 10^6 (Mat, 2011)	29
Figure 2.15	Round-edged wing flow separation (Peake and Tobak, 1980; Lang, 1998)	30
Figure 2.16	Possible separation line on round-edged wing flow separation (Jiang et al., 2000)	30
Figure 2.17	Medium-radius wing flow topology (Furman and Breitsamter, 2013)	31
Figure 2.18	Inner vortex on medium radius leading edge at R_{mac} = 3×10^6, α = 13° results from (i) experimental at DLR Gottingen, (ii) numerical solution of EADS Munich (Luckring and Hummel, 2013)	32
Figure 2.19	Simplified flow features of a rounded leading-edge Diamond wing	34
Figure 2.20	Incipient separation developing features (Frink et. al., 2016)	35
Figure 2.21	Flow visualisation of vortex flows for Λ=50° at (a) Re = 10^6, (b) Re = 13,000, (c) α = 7.5° (Gursul, 2004; Taylor, Schnorbus and Gursul, 2003)	37
Figure 2.22	Vortex flow structure system of diamond wing (Hitzel et. al, 2016)	38
Figure 2.23	Types of trip-dot/disturbance for forced transition (Buzica et. al., 2018)	41
Figure 2.24	Steady Surface pressure distributions (Hitzel et.al, 2016)	42
Figure 2.25	Turbulent vortex structures by ZDES prediction (Luckring et. al, 2016)	44
Figure 2.26	Turbulent kinetic energy fields by ZDES prediction (Deck, 2016)	45

Figure 2.27	Unsteady surface pressures by ZDES prediction (Luckring et. al, 2016)	46
Figure 2.28	Mean pressure distribution (Deck & Luckring, 2016).	47
Figure 2.29	Full model diamond wing (Hövelmann & Breitsamster, 2014)	50
Figure 2.30	Half model Diamond wing of Munich Technical University	52
Figure 2.31	The Installation of Diamond wing in Munich Technical University (Hövelmann et. al, 2016)	52
Figure 2.32	The results from PIV experiment in Munich University (Buzica & Breitsamster, 2019; Hövelmann et. al, 2016)	54
Figure 3.1	Flow of the research activities and methodology	58
Figure 3.2	Schematic of Universiti Teknologi Malaysia Low Speed Tunnel (UTM–LST) at UTM Aerolab	59
Figure 3.3	Final assembly of UTM delta wing model (Said, 2016)	60
Figure 3.4	Dimensions of NASA, Glasgow and UTM models (Said et. al, 2015)	61
Figure 3.5	SOLIDWORKS CAD drawing of UTM VFE-2 delta wing model (Said, 2016)	62
Figure 3.6	AVT-183 Diamond wing wind tunnel model configurations (Hovelmann, Knoth and Breitsamter, 2016)	63
Figure 3.7	Geometric of UTM Diamond wing model	65
Figure 3.8	Model assembly and components design	66
Figure 3.9	Component manufacturing and assembly	66
Figure 3.10	VFE-2 model installation for respective measurement in UTM-LST (Said, 2016; Tajuddin, 2021)	68
Figure 3.11	The off-surface pressure rake instrumentation (Tajuddin, 2021)	69
Figure 3.12	Pressure rake of KULITE dynamic pressure transducer in nine individual housing (Tajuddin, 2021)	70
Figure 3.13	Location of pressure rake at $Y/C_R = 0.3$ (Tajuddin, 2021)	70
Figure 3.14	UTM Diamond half-span testing system installed in UTM-LST	72
Figure 3.15	Steady balance data acquisition process flow	74
Figure 3.16	Unsteady balance data acquisition process flow	75

Figure 3.17	Tuft flow visualization testing	77
Figure 3.18	Camera positions outside test section for tuft flow visualization testing	78
Figure 3.19	Pressure taps locations on UTM Diamond wing	79
Figure 3.20	Surface pressure instrumentation	79
Figure 3.21	Surface pressures acquisition setup	80
Figure 3.22	Schematic diagram of complete experiment setup	82
Figure 3.23	PTS probe rod and transducer assembly	83
Figure 3.24	Off-surface measurement process flow	83
Figure 3.25	Off-surface measurement installed in test section	84
Figure 3.26	Measurement plane location	85
Figure 3.27	Grid notation of measurement points	86
Figure 3.28	Calibration process flow and setup	87
Figure 3.29	Linear sensor calibration	88
Figure 3. 30	Limitations for Off Surface Pressure Measurement	89
Figure 3.31	Kriging method (Bohling, 2005)	90
Figure 3.32	The contour mapping with application of Kriging estimation method (example from Bohling, 2005)	91
Figure 4.1	Forces and moments notation used in the experiment	94
Figure 4.2	Repeatability of lift, drag and pitching moment coefficient	95
Figure 4.3	Comparison of the C_L, C_D and C_M (UTM & TUM – AER)	96
Figure 4.4	Reynolds number effects on forces coefficient	98
Figure 4.5	C_L and CD trend	100
Figure 4.6	Reynolds number effects on pitching moment coefficient	101
Figure 4.7	Comparison of Diamond and VFE-2 for C_L, C_D & C_M $Re_{mac} = 2\times10^6$	103
Figure 4.8	Comparison of JR3 and Semi-span balance reading	106
Figure 4.9	Natural frequency experiment	107
Figure 4.10	Natural frequency of model structure	108
Figure 4.11	The effects of angle of attack on data spectra at Re= 3×10^6	111
Figure 5.1	Flow visualization at (a) $\alpha=0°$ and (b) $\alpha = 6°$ for Re=1×10^6	114

Figure 5.2	Flow pattern at (a) α = 9° and (b) α = 12° for Re = 1×10^6	115
Figure 5.3	Flow pattern at α = 15° for Re = 1×10^6	116
Figure 5.4	Flow visualization at (a) α = 18° and (b) α = 24° for Re = 1×10^6	117
Figure 5.5	Flow pattern at (a) α = 6° and (b) α = 9° for Re = 2×10^6	118
Figure 5.6	Flow pattern at (a) α = 12° and (b) α = 13° for Re = 2×10^6	119
Figure 5.7	Flow pattern at (a) α = 15°, (b) α = 18° and (c) α = 24° for Re = 2×10^6	120
Figure 5.8	Flow pattern at (a) α = 6°, (b) α = 9° and (c) α = 12° for Re = 3×10^6	122
Figure 5.9	Flow pattern at (a) α = 15°, (b) α = 18° and (c) α = 24° for Re = 3×10^6	123
Figure 5.10	Flow pattern at on sharp-edged delta wing at α = 12°, Re_{mac} = 1×10^6 (Kasim, 2017)	124
Figure 5.11	Tuft flow pattern on large-edged VFE-2 wing model at α = 12° and Re_{mac} = 1×10^6 (Tajuddin, 2021)	125
Figure 6.1	The installation of NATO Diamond wing in TUM-AER (Buzica & Breisamter, 2019)	128
Figure 6.2	Reynolds number effects of surface Cp distributions between works from NATO Group at Re_{mac} = 2.7×10^6 and UTM at Re_{mac} = 2×10^6 at α = 12°.	129
Figure 6.3	On – surface spanwise Cp distributions with varied Re at α = 6°	131
Figure 6.4	On – surface spanwise Cp distributions with varied Re at α = 9°	132
Figure 6.5	Detail view of spanwise Cp distributions at x/c_R = 0.2, x/c_R = 0.3 and x/c_R = 0.4 at α = 9°.	133
Figure 6.6	On – surface spanwise Cp distributions with varied Re at α = 12°	135
Figure 6.7	On – surface spanwise Cp distributions with varied Re at α = 15°, and at α = 27° for Re = 3×10^6	137
Figure 6.8	Pressure distributions for large leading-edged delta wing VFE-2 configuration at α = 21°	138
Figure 6.9	Reynolds number effects of leading-edge pressures for angle of attack trend analysis	140

Figure 6.10	Reynolds number effects of pressure distribution along the leading edge at (a) α = 6°, (b) α = 9° and (c) α = 12°	142
Figure 6.11	Comparison of leading-edge pressures on three wings at x/cR = 0.5 and (a) Re_{mac} = 1×10^6 (b) Re_{mac} = 2×10^6	144
Figure 6.12	Comparison of leading-edge pressures on three wings at x/cR = 0.2 and (a) Re_{mac} = 1×10^6 (b) Re_{mac} = 2×10^6	145
Figure 6.13	Surface pressure contours at Re = 3 ×10^6 for angle of attack effects	147
Figure 6.14	Detail views of local surface pressures contour at Re = 3 ×10^6 and (a) α = 9°, (b) α = 12°.	149
Figure 6.15	Reynolds number effects of pressures contour at (a) α = 9°, (b) α = 12°, and (c) α = 18°.	150
Figure 6.16	Comparison between (a) $R_{mac} = 1 \times 10^6$ and (b) $R_{mac} = 2 \times 10^6$ for medium-edged wing at α = 13.3°	152
Figure 6.17	Coordinate system used to interpret the off-surface results	154
Figure 6.18	Angle of attack effects at Re = 1×10^6, x/c_R = 0.4	156
Figure 6.19	Angle of attack effects at Re = 2×10^6, x/c_R = 0.4	158
Figure 6.20	Angle of attack effects at Re = 2×10^6, x/c_R = 0.5	160
Figure 6.21	Angle of attack effects at Re = 3×10^6, x/c_R = 0.4	162
Figure 6.22	Angle of attack effects at Re = 3×10^6 and three chord-wise section, x/c_R = 0.4, 0.5 and 0.6	164
Figure 6.23	Details localize pressure at Re = 3×10^6, α = 6º, and x/c_R = 0.6	165
Figure 6.24	Details localize pressure at Re = 3×10^6, α = 9º, and (a) x/c_R = 0.4, (b) x/c_R = 0.5, (c) x/cR = 0.6.	166
Figure 6.25	Details localize of Reynolds number effects at α = 9° and three chord-wise section, x/c_R = 0.4, 0.5 and 0.6	168
Figure 6.26	Details localize of Reynolds number effects at α = 12° and three chord-wise section, x/c_R = 0.4, 0.5 and 0.6	169
Figure 6.27	The pressure contour for Y/Cr = 0.4 at medium-edged wing and Re_{mac} = 1×10^6	171
Figure 6.28	The pressure contour for Y/Cr = 0.3 at large-edged wing and α = 18°	172
Figure 6.29	Vortices above delta-shaped Diamond Wing	173
Figure 6.30	The illustration of primary vortex structural difference	174

LIST OF ABBREVIATIONS

AVT	-	Advance Vehicle technology
CAD	-	Computer-Aided Design
CFD	-	Computational Fluid Dynamics
DLR	-	German Aerospace Center
EADS	-	European Aeronautic Defense and Space
GPS	-	Global Positioning System
HWA	-	Hot Wire Anemometry
LTPT	-	Low Turbulent Pressure Tunnel
NACA	-	National Advisory Committee for Aeronautics
NASA	-	National Aeronautics and Space Administration
NATO	-	North Atlantic Treaty Organisation
NLR	-	National Langley Research
NTF	-	National Transonic Facility
PIV	-	Particle Image Velocity
PSI	-	Static surface pressure
PSP	-	Pressure Sensitive Paint
RTO	-	Research & Technology Organisation
SACCON	-	Stability And Control CONfiguration
SOLIDWORKS	-	a CAD software
TUM-AER	-	Technical University of Munich -
UAV	-	Unmanned Aerial Vehicle
UCAV	-	Unmanned Combat Air Vehicle
UTM	-	Universiti Teknologi Malaysia
UTM-LST	-	Universiti Teknologi Malaysia Low Speed Tunnel
VFE	-	Vortex Flow Experiment
ZDES	-	Zonal Detached Eddy Simulation

LIST OF SYMBOLS

α	-	Angle of attack
η	-	span-wise ratio distance from mid-wing to local semi spans length
ρ	-	Air density
Λ	-	Swept angle
Λ_{le} ; φ_{le}	-	Leading edge swept angle
Λ_{te} ; φ_{te}	-	Trailing edge swept back angle
b	-	Wing maximum span
C_R ; C_r	-	Wing Root Chord
$\bar{c}$; c_{mac}	-	Mean Chord
C_L ; C_D ; C_M	-	Lift Coefficient ; Drag Coefficient ; Pitching Moment Coefficient
C_P ; $C_{p,le}$	-	Pressure coefficient ; Leading edge pressure coefficient
h_{stan}	-	Stand-off height
r_{le}/c	-	Leading edge radius to local chord ratio
x/c_R	-	Chord-wise location
x_{MRP}	-	Moment Reference Point in chord-wise location
y/s	-	Span-wise location
AR	-	Wing Aspect Ratio
BMC	-	Balance Moment Centre
F	-	Force
M	-	Moment
Re	-	Reynolds Number based on root chord
Re_{mac} ; R_{mac}	-	Reynolds number at mean aerodynamic chord
P	-	Pressure
S	-	Planform area
U_∞	-	Freestream
v	-	Velocity

LIST OF APPENDICES

APPENDIX	TITLE	PAGE
Appendix A	Pressure Taps Locations	193
Appendix B	KULITE XCL-072 Data Sheet	199
Appendix C	VFE-2 Delta Wing and Sting Profile	201
Appendix D	Moment Rotation Point (MRP) Calculation	205

CHAPTER 1

INTRODUCTION

1.1 Introduction

Delta wing is a triangle planform when it views from the top projection. The words ‘delta’ is named after it similarity shape with the Greek uppercase letter delta (Δ). When the air flowed through a delta wing at certain angle of attack and speeds, the flow will separate and generate a pair of vortex on the upper surface of the wing. The generated vortices induce suction forces that can increase the wing lift coefficient (Polhamus, 1966). Vortex flow phenomena above delta wing is very complicated, unresolved and has been studied for many years.

The aerodynamic characteristics of the sharp-edged delta wing have been studied comprehensively in many years. The main flow structure observed on the upper surface is the leading edge vortex. At certain angle of attack, the separation occurs at the leading edge and its rolls up to form leading edge or primary vortex as described by Hummel (1979). This vortex travel downstream and has increased negative suction peak on the upper, this situation will increase the lift coefficient.

There are many other flow phenomena for sharp-edged delta wing such as vortex breakdown, vortex interaction and shock vortex interaction have been documented by Lambourne & Bryer (1961), Mitchell (2003), Hall (1998), Schiavetta et al. (2009) and Miller & Wood (1985) works. However, the flow topology above the wing will change if the leading is blunt.

In practice, blunt leading edge profile is more favourable in aircraft design especially in UAV and UCAV application. The primary vortex for the blunt-edged wing behaves differently compared to the sharp wing. The primary vortex developed at certain chordwise from the wing apex, Luckring (2004; 2010; 2019). The bluntness

has caused the vortex becomes smaller, weaker and it located further outboard of the wing.

Throughout the past decades, delta wing has found to be a profile for high manoeuvre combat aircraft including UAV (Unmanned Air Vehicle) and UCAV (Unmanned Combat Air Vehicle). There are two types of delta wing, which is associated to UAV or UCAV applications, the first one is slender wing and the second type is the non-slender wing. Slender delta wing is for wing profile that have the swept angle more than 60° while non-slender delta wing has angle less than 60° as illustrated in Figure 1.1.

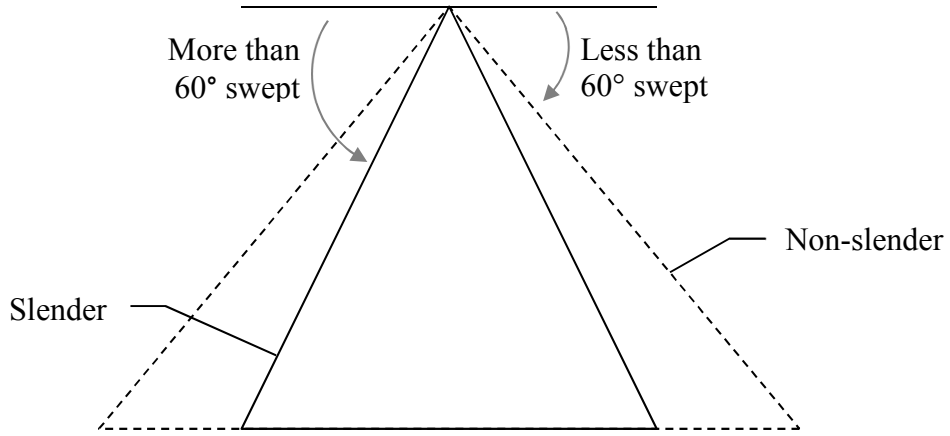

Figure 1.1 Slender vs. non-slender types of Delta wing

One of the advantages for delta shape is the wing can achieve high speed at certain flight conditions (Luckring, 2010; Pevitt & Alam, 2014). The non-slender wing also become an important area in aerodynamic research recently. There are different type of delta wings that can be applied for UAC and UCAV aircraft. They can be either tailed or tailless, cropped or compound, cranked or Ogival, lambda or diamond delta's wing. These different types of delta configurations are illustrated in Figure 1.2.

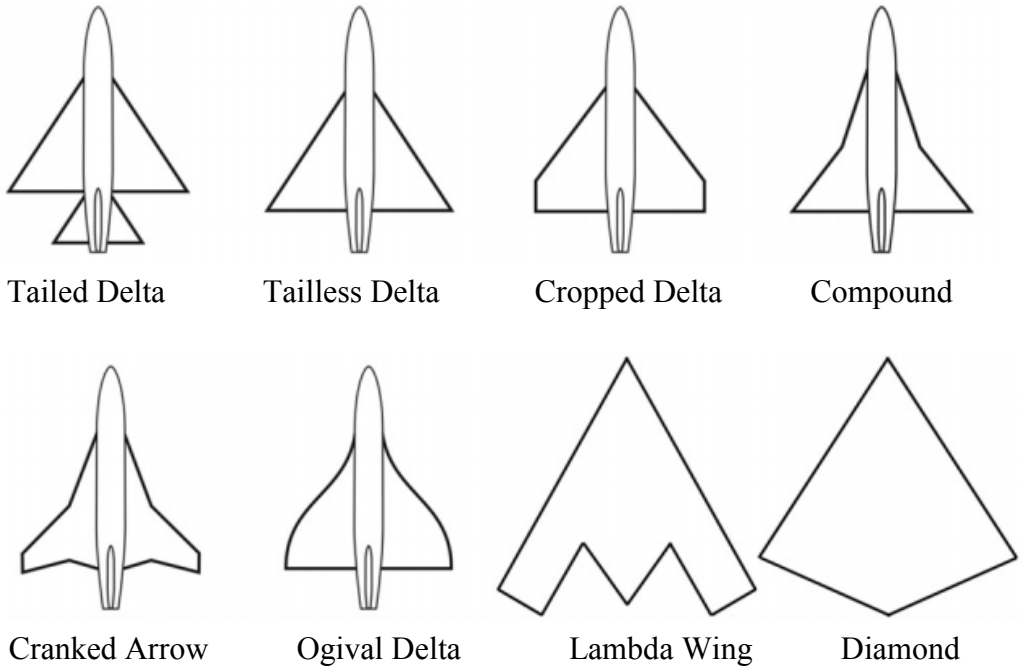

Figure 1.2 Types of Delta wing configurations (Pevitt and Alam, 2014)

There are many types of UAVs, each of them is depends on the mission and application required. The flight range also depends on the Reynolds number of a mission as shown in Figure 1.3. For example, the operating Reynolds number for UCAV is up to 10^7.

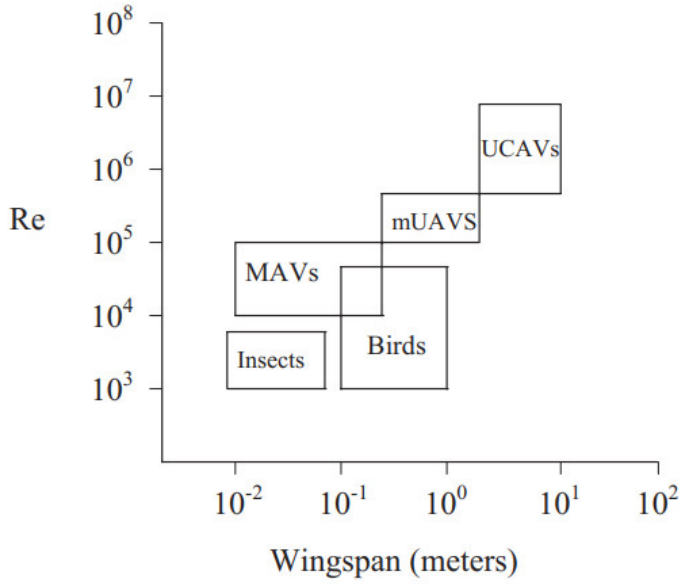

Figure 1.3 Reynolds number range for UAV (Gursul, 2004)

There are several aircraft UCAV programmes around the globe as shown in Figure 1.4. Most of the UCAV design incorporated with the lambda wing planform with highly blended wing design. Modern UCAV configurations preferred to use medium to highly swept wings with either rounded or variable leading edge geometries (Schütte, 2016). Highly blended flying wing designs commonly used to achieve a stealthy and agile attribute, which are one of the key technologies affecting the UCAV design (Sepulveda & Smith, 2017). This is mainly due to the stealth requirements and its mission priority (Sepulveda & Smith, 2017). One of the problem with the delta wing aircraft configurations are having nonlinear aerodynamic characteristics (Polhamus, 1966) due to the complex vortical flow above the wing. More numerical and experimental data are needed to understand the flow topology above the wing.

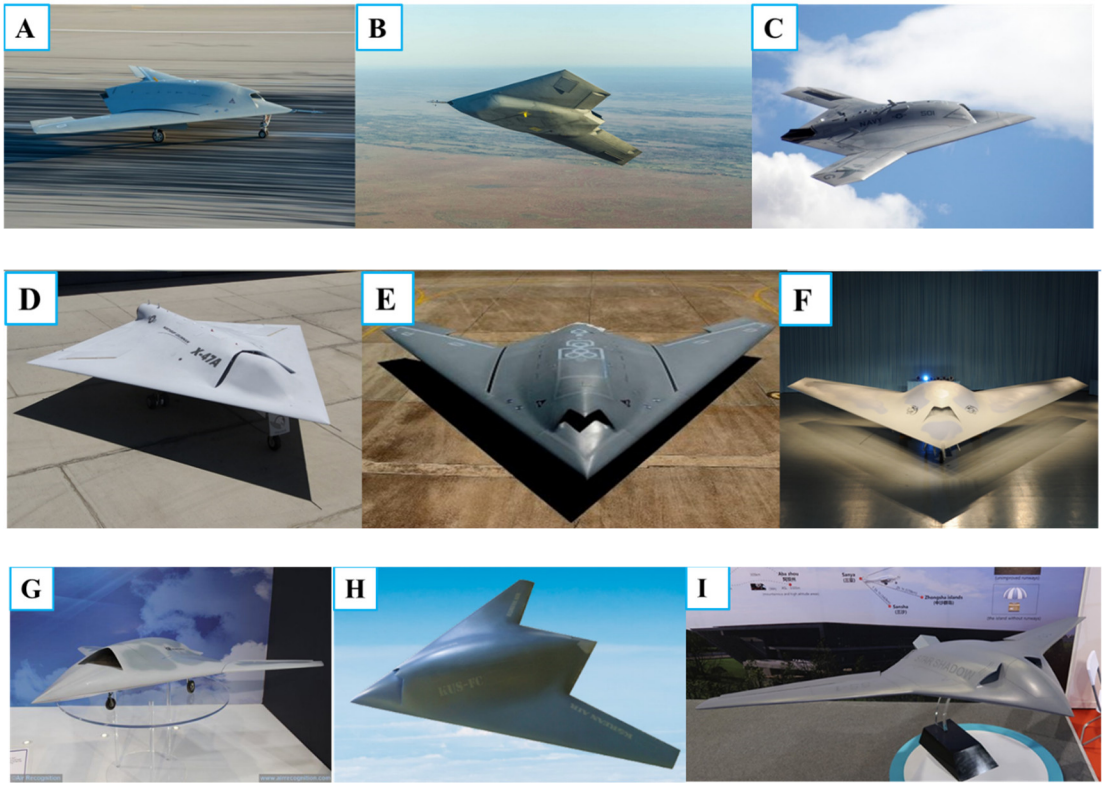

Notes: *A = Dassault nEUROn (Dassault Aviation, 2018); B = Taranis (BAE Systems, 2018); C = X-47B (Northrop Grumman Corporation, 2018); D = X-47A Pegasus (Defense Advanced Research Projects Agency, 2001); E = AURA UCAV (Indian Defence Update, 2018); F = Phantom Ray Demonstrator (Boeing, 2010); G = K-X UCAV (Air Recognition, 2017); H = KUS-FC (Korean Air Tech Centre, 2016); I = Star Shadow (Minnick, 2018).*

Figure 1.4 Current and future UCAV design

Based on several considerations, diamond-shaped has been chosen as one of the planform for UCAV design. One of the UCAVs that will be used in the future is diamond-shaped profile as shown in Figure 1.5. It was developed by the Northrop Corporation Company namely X – 47A. Therefore, this thesis has focused on the dethe diamond shaped wing.

Figure 1.5 Diamond shaped X-47A UCAV

To focus on UCAV and delta wing related research, NATO has established several research groups under the AVT (Advance Vehicle technology) organization. There are several research series with different objectives under the AVT.

Among the first facet was the AVT–113 group that was established in 2002. This group is called the Vortex Flow Experiment Two (VFE-2). The aims of this team were to increase technology readiness for the military knowledge and for future aircraft wing (Lamar & Hummel, 2008). One of the main objectives of AVT–113 is to focus on a flat delta wing with different leading edge profile. The wing has the swept angle of 65°. This VFE-2 group re-uses the NASA delta wing model tested in 1997 as a platform to understand the flow characteristics of delta wing. The profile and wind tunnel set up are as shown in Figure 1.6. The main objectives of this NATO working group were to investigate the effects of leading edge bluntness, angle of attack, Reynolds number and Mach number on the vortical flow above slender delta-shaped wing of 65° swept angle (Chu & Luckring, 1996; Luckring 2013; Lamar & Hummel, 2008).

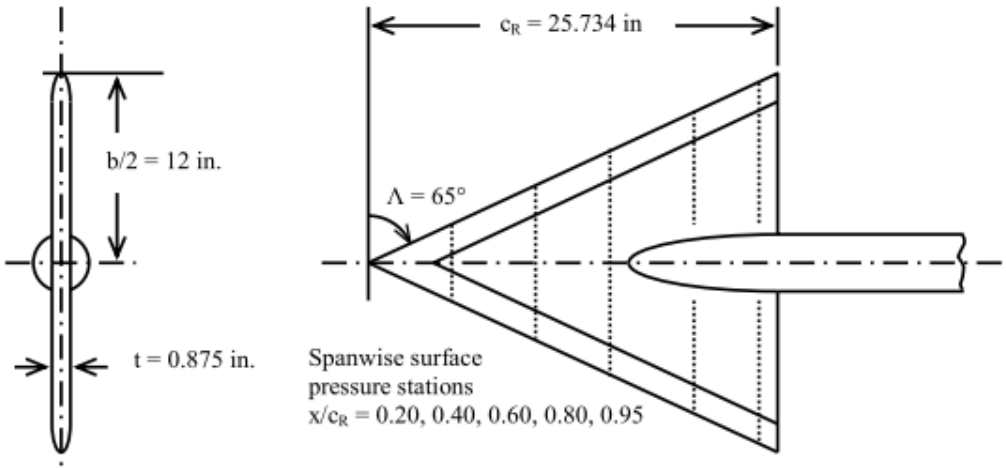

(a) The VFE-2 profile of NASA 65° delta wing

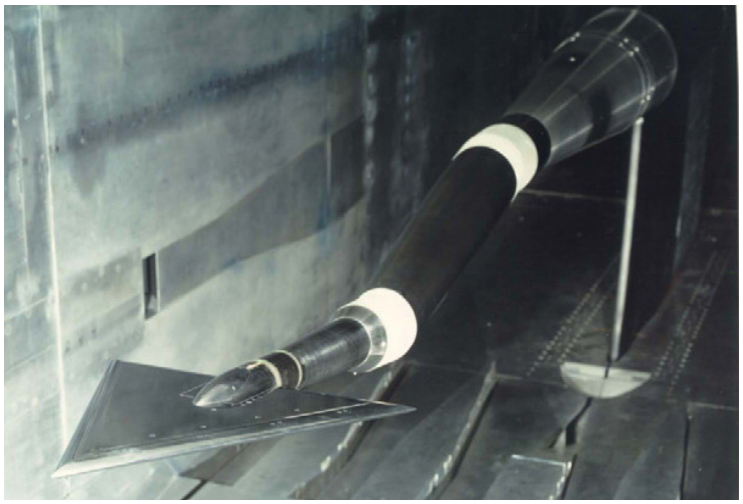

(b) The installation of VFE-2 delta wing in NASA Langley Research Center

Figure 1.6 The AVT-113 experimental model and testing in NASA wind tunnel (Luckring, 1996)

During the campaign, several experimental and numerical works were performed on 65° delta wing across the European wind tunnels and CFD centres. The results obtained from the blunt-edged delta wing were compared with those from the sharp leading edge wing. The result from this experiment provides the knowledge on the starting point of separation, location of the primary vortex and vortex breakdown that can guide the numerical group to improve the numerical calculations (Lamar & Hummel, 2008). For the blunt-edged wing, the flow separation is no longer fixed at the leading edge, thus the flow is dependent on the Reynolds numbers (Hummel, 2008). At certain speeds and high angle of attack, the vortical flow became more complicated to be predicted experimentally or numerically. These projects ended in

2010 and several hypotheses were made and well documented (Hummel, 2008; Luckring, 2013; Luckring and Hummel, 2013). This VFE-2 profile has become as a *standard* platform for the delta wing profile developed by NATO recently.

Continuing from the AVT–113 tasks, recently, several other AVT were established to investigate a higher complexity level of unit problems in vortical flow on delta shaped wing, the most related to the UCAV development were the NATO AVT–161 and AVT–183. The Task Group AVT–161 was formed to perform the aerodynamic research on the complex profiles called SACCON configurations. SACCON is a proposed planform for the NATO to venture into the Uninhabited Combat Air Vehicle (UCAV), shown in Figure 1.7. The SACCON configuration was design to incorporate some design features from the industry.

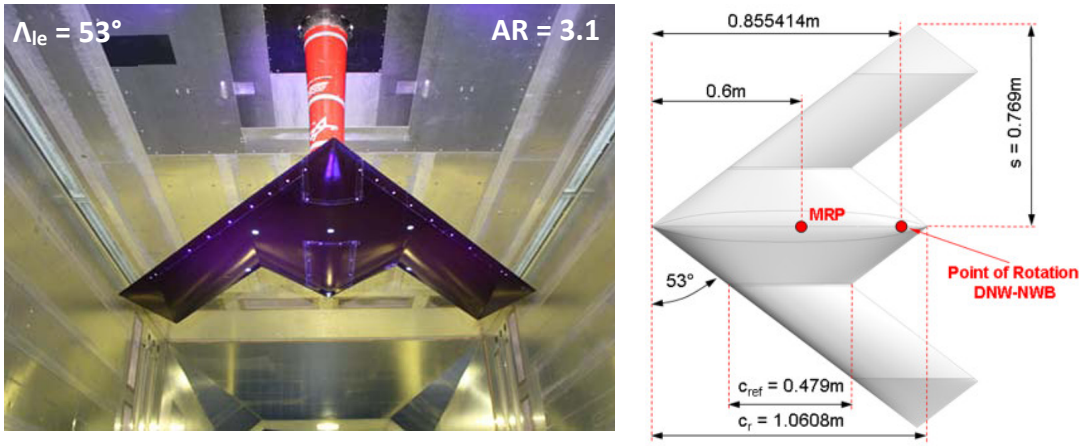

Figure 1.7 AVT-161 SACCON model and configurations (Cummings and Schütte, 2012)

The group has found that the flow fields around the wing were found to be very complex that involved many interacting vortical flows as in Figure 1.8 (Cummings & Schütte, 2012; Cummings, Liersch and Schütte, 2018). Several problems cannot be solved such as transition location mid board of the wing by Numerical or experimentally during the AVT–161.

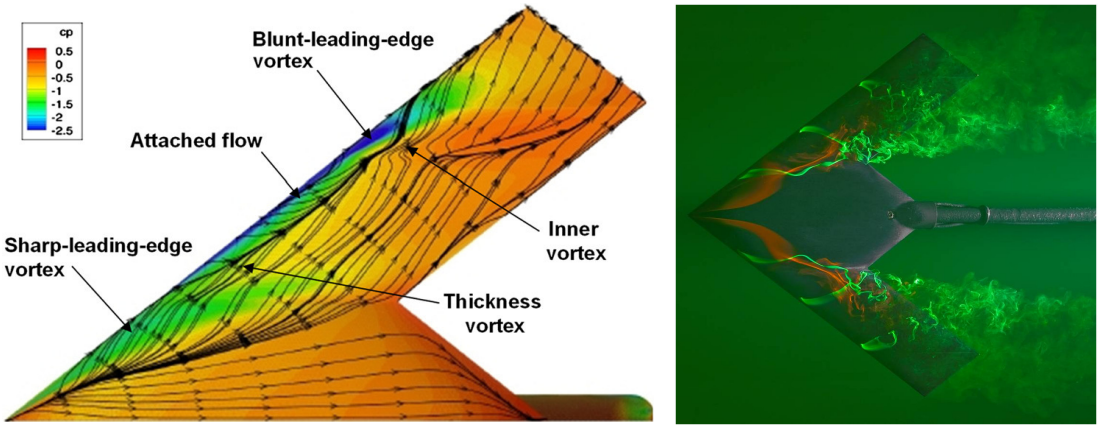

Figure 1.8 Complex SACCON flow field (Fink, 2010; Cummings and Schütte, 2012)

In order to reduce the complexity from the SACCON wing, the NATO research team has designed a reduce-complexity model so the targeted area can be focused. To relate the different level of complexity of that framework, the NATO used hierarchical decomposition method as shown in Figure 1.9 (Luckring et al., 2016).

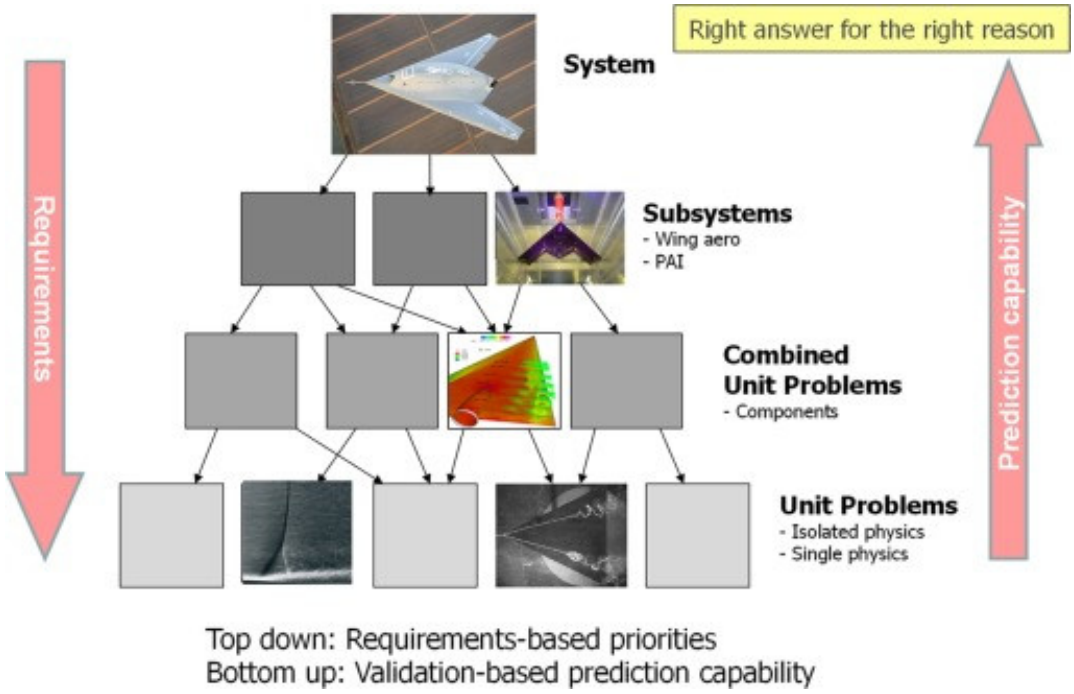

Figure 1.9 NATO hierarchical decomposition of aerodynamic complexity connection to SACCON (Luckring et al., 2016)

In order to reduce the complexity of the SACCON wing, another NATO research group has been established, AVT–183. A simplified model called Diamond was introduced. The profile of the Diamond wing was derived from the SACCON configuration with similar wing swept angle as shown in Figure 1.10. The data obtained from the diamond wing should provide a better insight into the complexity of the SACCON wing. Therefore, the Diamond wing was used to provide the fundamental flow physics for the complicated SACCON profile.

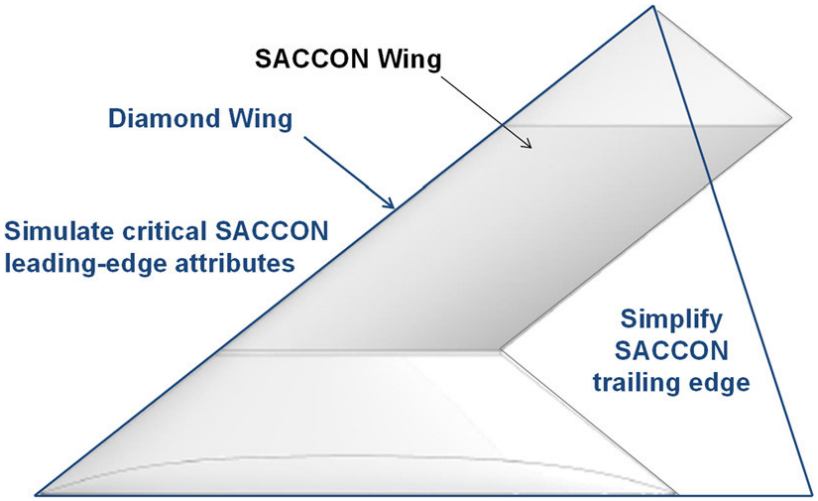

Figure 1.10 AVT-183 Diamond wing configuration as simplified AVT-161 SACCON (Luckring et. al., 2016)

Diamond is a non-slender wing that has blunt 53° swept angle and trailing edge swept angle -26.5° with a constant NACA 64A006 aerofoil across the wing (Luckring et. al., 2016). The task group will further investigate the detailed development of the primary vortex in the leading-edge area, details interaction between the primary vortex and the inboard inner vortex. Also to improve the Numerical prediction on both planforms (Hövelmann & Brietsamter, 2014; Luckring & Boelens, 2011).

The first experimental work on Diamond was performed in The Institute of Aerodynamics and Fluid Mechanics Technische Universität München (TUM-AER) (Hövelmann, & Breitsamter, 2012; 2014). The initial results has shown that the interacting vortical flow also happened on Diamond wing.

The AVT-183 research was focused on constant airfoil Diamond wing. Besides the advantage of the potential lift induced inboard of the wing, the main advantage of diamond wings is that the induced lift produced by the vortex in the leading-edge area can enhance the aircraft longitudinal static stability. The future work will include experimental investigations to help distinguish modelling requirements for successful prediction of blunt leading-edge vortex separation relevant to Diamond wing. The correct prediction of Diamond wing configuration would not only can improve the understanding of the aerodynamics of diamond-shape planform itself but it would also be a prerequisite to model other SACCON-relevant vortex phenomena and their aerodynamic effects.

1.2 Problem Statement

Aerodynamics characteristics is one of the importance factors in aircraft design process. It is more difficult to design Diamond-shaped UCAV aircraft because the flow field above the upper surface is known to be very complicated. The complexity of the flow particularly in the leading edge increases when the leading edge is rounded. The non-slender type of Diamond-shaped wing is also a derivation from the delta wing configuration. At higher angle of attack, the flow is extremely complicated and unresolved.

As has been explained, the experimental data for VFE-2 configuration (classified as slender wing) has been well documented and has a distinct contribution to the CFD simulation to well predict the vortical flow above the VFE-2 standard delta wing (Hummel & Cummings, 2013). The similar developed turbulent model were used to simulate the aerodynamic characteristics and performances of Diamond wing has shown some discrepancy in the calculation (Hitzel et al., 2016; Luckring, 2019). This discrepancy was due to the input information used in the development of the turbulent model is based on the information on the VFE-2 configuration which is an isolated unit problem. For the Diamond wing, it is a combined unit problem.

The numerical calculation can be improved by the comprehensive data provided by wind tunnel experiment. However, the experimental data for Diamond wing configuration is not well documented when compare to the VFE-2 configuration. Most of the published data was found to be limited to the primary vortex in the leading-edge region only. However, the flow above the Diamond wing consists of several other structures. According to Luckring et. al. (2016), the main flow structure above the Diamond wing configurations are (i) incipient separations; a region where the boundary layer near the leading edge initiates the leading-edge vortex, (ii) primary vortex, (iii) secondary vortex, (iv) attached flow and (v) inner vortex. This complicated flow topology may be due to the effect of configuration. Beside the primary vortex, the flow structures inboard of the wing is consisted with another vortex called is as the *inner vortex*. The information of this vortex is still limited to date. More wind tunnel experiments are needed to improve the understanding of the inboard structures formation, progression and the vortical flow interaction.

More wind tunnel experiments are needed in order to obtain the flow topology on the upper surface of the Diamond wing particularly the inner vortex and flow in the inboard region. Information of the flow physics such as the distribution pattern of the airflow, the pressure distribution, the shear layer structures, the location of vortices onset, size and its intensity are the substantial data for the improvement of the turbulent model. This information would have improved the numerical calculation and prediction of the blunt-edged Diamond wing configuration aerodynamic characteristics and performances.

1.3 Research Objectives

The research objectives of this project are:

1. To identify the vortical structures on diamond wing configuration using experimental approaches.

2. To investigate the effects of angle of attack and Reynolds number variation on the detail development and interaction of the primary and inner vortices.

3. To perform physical measurements on the vortical flow structures properties above the Diamond wing and in particular the inner vortex inboard of the wing.

1.4 Research Scope

To achieve the objectives, the scope of this thesis are:

1. The research investigation is conducted using experimental approach only. All the experiment is carried out in UTM Aerolab facility using UTM-LST wind tunnel. The selection of the experimental method conducted was based on the available test equipment and instrumentations with their respective limits.

2. The model was designed to meet 53° sweep Diamond wing with rounded leading-edge model as provided by the NATO AVT-183 group. The size of the model fabricated in UTM is scaled 1:1 to the model in Munich Technical University.

3. All the test experiments were conducted in static state wind tunnel test.

4. The experiments were carried out in atmospheric air as working conditions and flow was assumed to be incompressible at three Reynolds number conditions in subsonic region.

5. The experiments were also carried out to investigate the effects of Reynolds Numbers of 1×10^6, 2×10^6, and 3×10^6 based on wing chord. These Reynolds

Number conditions were selected to represent the transitional flow conditions during the take-off and landing.

6. This Diamond wind tunnel model was fabricated at similar size to the actual Diamond wing UCAV proposed by the NATO group. Therefore, the similarity test is not conducted in this study.

7. The aerodynamic longitudinal static stability was investigated by pitching the model angle of attack ranges from 0° to 30° with increments of 3°. The pitching angles are expected can fulfilled all ranges of flight condition. However, the maximum angle of attack tested may differ from the experiments carried out by the NATO group which mainly due to the physical constraint of UTM Aerolab.

8. All the investigations were measured on the upper surface of the wing only. The flow on lower surface of the wing is not in the scope.

9. For the off-surface measurement, the investigation were made at selected three position, $X/C_r = 0.4, 0.5, 0.6$ and at selected angle of attack 6°, 9°, 12°, 15° and 18° only. At this angle of attack, the desired inboard flow separation occurs for all Reynolds number cases.

1.5 Significance of the study

The flow above Diamond wing is not fully understood. On the upper surface of the wing, the primary vortex developed in the leading edge while the inner vortex developed inboard of the wing. The detail interaction between the primary and the inner vortex is not well explained. The flow further inboard of the wing is also not available to date. This thesis will provide the detail interaction between these vortices and also the flow topology inboard of the wing. The information gathered from this study would be valuable for an accurate prediction of vortical flow above diamond-relevant planform.

REFERENCES

Abdullah, M. F. (2018) *Influences of active flow control techniques on vortex properties above blunt-edged delta wing*. Master Thesis, Universiti Teknologi Malaysia, Skudai.

Airforce Technology (n.d.) *X-47 Pegasus UCAV*. Available at: https://www.airforce-technology.com/projects/x47/ (Accessed: 5 February 2021).

Anderson, Jr. J. D. (2001) *Fundamentals of Aerodynamics.* International Edition. New York: McGraw-Hill Higher Education. ISBN 0-07-118146-6.

Ashifkhan (n.d.) *What is downwash and upwash in airfoil?* Photograph. Available at: https://qph.fs.quoracdn.net/main-qimg-18888cbc71dde3a6d1ac29f243f9dc44.webp (Accessed: 16 November 2017).

Ball, M. (2017) *Airbus Jet-Propelled UAV Demonstrator Completes First Test Flight*. Available at: https://www.unmannedsystemstechnology.com/2017/07/airbus-jet-propelled-uav-demonstrator-completes-first-test-flight/ (Accessed: 5 February 2021).

Barlow, J. B., Rae, Jr. W. H. and Pope, A. (1999). *Low-speed Wind Tunnel Testing*. (3rd ed.). New York: John-Wiley & Sons.

Bohling, G. (2005). *Kriging*. Unpublished note, Kansas Geological Survey, Kansas University.

Brett, J. and Ooi, A. (2014) 'Effect of sweep angle on the vortical flow over Delta wings at an angle of attack of 10°', *Journal of Engineering Science and Technology*, 9(6), 768-781.

Buchholz, M. D. and Tso, J. (2000) 'Lift Augmentation on Delta Wings with Leading-Edge Fences and Gurney Flap', *Journal of Aircraft*, 37(6), pp. 1050-1057.

Buzica, A. Debschütz, L., Knoth, F. and Breitsamter, C. (2018) 'Leading-Edge Roughness Affecting Diamond-Wing Aerodynamic Characteristics', *Aerospace*, 5(3), 98. doi: 10.3390/aerospace5030098.

Buzica, A. and Breitsamster, C. (2019) 'Turbulent and transitional flow around the AVT-183 diamond wing', *Aerospace Science and Technology,* 92, 520-535.

Buzica, A., Bartasevicius, J. and Breitsamster, C. (2016) Active vortex flow control on a generic delta wing. In *30th Congress of the international Council of the Aeronautical Sciences*. 25-30 September. Daejeon, Korea : ICAS2016_0257.

Cipolla, K. M. and Rockwell, D. (1995) 'Flow Structure on Stalled Delta Wing subjected to Small Amplitude Pitching Oscillations', *AIAA Journal*, 33(7), pp. 1256-1262

Chu, J. and Luckring, J. M. (1996) *Experimental Surface Pressure Data Obtained on 65° Delta Wing across Reynolds Number and Mach number Ranges, Vol. 1-4, Sharp, Small, Medium, Large Leading Edge*. NASA Technical Memorandum 4645.

Coton, F. N., Mat, S. and Galbraith, R. (2008) *Chapter 22 – Experimental Investigations on the VFE-2 Configurations at Glasgow University*. RTO-TR-AVT-113.

Cummings, R. M, Liersch, C. M. and Schütte, A. (2018) Multi-Disciplinary Design and Performance Assessment of Effective, Agile NATO Air Vehicles. In *Applied Aerodynamics Conference*. 25-29 June. Atlanta, Georgia: AIAA2018-2838.

Cummings, R. M. and Schütte, A. (2012) 'Integrated computational/experimental approach to unmanned combat air vehicle stability and control estimation'. *AIAA Journal of Aircraft,* 49(6), 1542–1557.

Deck, S. (2012) 'Recent improvements in the Zonal Detached Eddy Simulation (ZDES) formulation', *Theoretical and Computational Fluid Dynamics,* 26(6), 523–550.

Deck, S. (2012b) 'Zonal detached eddy simulation of the flow around a high-lift configuration', *AIAA Journal,* 43(11), pp. 2372–2384.

Deck, S. and Luckring, J. M. (2016) 'Zonal Detached Eddy Simulation (ZDES) of the flow around the AVT-183 diamond wing configuration', *Aerospace Science and Technology,* 57, 43–51. doi: 10.1016/j.ast.2016.02.020.

Deck, S., Gand, F., Brunet, V., Khelil, S. B. (2014) 'High-fidelity simulations of unsteady civil aircraft aerodynamics: stakes and perspectives. Application of zonal detached eddy simulation', *Philosophy Transaction Royal Society A*, 372: 20130325. doi: 10.1098/rsta.2013.0325

Dehpanah, P. and Nejat, A. (2015) 'The aerodynamic design evaluation of blended-wing-body configuration', *Aerospace Science and Technology*, 43, 96-110.

Dole, C. E. and Lewis, J. E. (2001). *Flight Theory and Aerodynamics, A Practical Guide for Operational Safety*. (2nd ed.). United States of America : John Wiley & Sons, Inc.

Earnshaw, P. B. (1962) *An Experimental Investigation of the Structure of a Leading-Edge Vortex*. Aeronautical Research Council Reports and Memoranda, No. 3281.

Fink, P. T. (1966) *Some Early Experiments on Vortex Separation, Part 1: Some Low Speed Aerodynamic Properties of Cones*. Aeronautical Research Council Reports and Memoranda, No. 3489.

Fletcher, H. S. (1958) *Low-speed experimental determination of the effects of leading-edge radius and profile thickness on static and oscillatory lateral stability derivatives for a delta wing with 60 degrees of leading-edge sweep.* Washington : Technical note / National Advisory Committee for Aeronautics, NACA TN No. 4341.

Frink, N. T. (2010) Strategy for dynamic CFD simulations on SACCON configuration. In *28th AIAA Applied Aerodynamics Conference*. 28 June - 01 July. Chicago, Illinois : AIAA 2010-4559.

Frink, N. T., Tomac, M. and Rizzi, A. (2016) 'Collaborative study of incipient separation on 53° -swept diamond wing', *Aerospace Science and Technology*, 57, 76 –89.

Fritz, W. (2008) *Chapter 25 – Numerical Solutions for the VFE-2 Configurations on Structured Grids at EADS-MAS, Germany*. RTO-TRAVT-113 : 25-1 – 25-21.

Fritz, W. (2013) 'Numerical Simulation of The Peculiar Subsonic Flow-field About The VFE-2 Delta Wing with Rounded Leading Edge', *Aerospace Science and Technology*, 24(1), 45 - 55.

Fritz, W. and Cummings, R. M. (2008) *Chapter 34 – Lessons Learned From the Numerical Investigations on the VFE-2 Configuration*. RTO-TR-AVT-113 : 34-1 – 34-31.

Furman, A. and Breitsamter, C. (2008) *Chapter 21 – Experimental Investigations on the VFE-2 Configurations at TU Munich, Germany*. RTO-TR-AVT-113.

Furman, A. and Breitsamter, C. (2013) 'Turbulent and Unsteady Flow Characteristics of Delta Wing Vortex Systems', *Aerospace Science and Technology,* 24(1), 32 – 44.

Gad-El-Hak, M. and Blackwelder, R. F. (1985) *The discrete Vortices from a Delta Wing*. Technical Report : 23, 961-962.

Ghazijahani, M. S. and Yavuz, M. M. (2019) 'Effect of thickness-to-chord ratio on aerodynamics of non-slender Delta wing', *Aerospace Science and Technology*, 88, 298-307.

Ghoreyshi, M., Ryszka, K. J., Cummings, R. M., Lofthouse, A. J. (2016) 'Vortical flow prediction of a diamond wing with rounded leading edges', *Aerospace Science and Technology*, 57, 103–117.

Gordnier, R. E. and Visbal, M. R. (2003) Higher-order compact difference scheme applied to the simulation of a low sweep delta wing flow. In *41st Aerospace Sciences Meeting and Exhibit*. 6-9 Jan. Reno, Nevada : AIAA 2003-0620.

Gursul, I. (2004) 'Recent developments in delta wing aerodynamics', *The Aeronautical Journal*, 108(1087), 437- 452.

Gursul, I. (2005) 'Review of unsteady vortex flows over slender delta wings', *Journal of Aircraft,* 42(2), 299-319.

Gursul, I., Gordnier, R., and Visbal, M. (2005) 'Unsteady aerodynamics of nonslender delta wings', *Progress in Aerospace Science*, 41(7), 515–557. doi: 10.1016/j.paerosci.2005.09.002.

Hadidoolabi, M. and Ansarian, H. (2017) 'Supersonic flow over a pitching delta wing using surface pressure measurements and numerical simulations', *Chinese Journal of Aeronautics*, 31(1), 65-78.

Hall, R. M. (1998) Impact of Fuselage Cross Section on the Stability of Generic Fighter. In *16th AIAA Applied Aerodynamics Conference.* 15-18 June. Albuquerque, New Mexico: AIAA98-2725, 515-525.

Hamizi, I. B. and Khan, S. A. (2019) 'Aerodynamics investigation of Delta wing at low reynold's number', *CFD Letters*, 11(2), 32-41.

Henderson, W.P. (1976) *Effects of Wing Leading-Edge Radius and Reynolds Number on Longitudinal Aerodynamics Characteristics of Highly Swept Wing-Body Configurations at Subsonic Speeds*. NASA Technical note. TN–D–8361.

Hitzel, S. M. (2013) Perform and Survive – Evolution of Some U(M)CAV Platform Requirements. In *STO AVT Workshop on Innovative Control Effectors for*

Military Vehicles. 20 – 22 May. Stockholm, Sweden: No.1, STO-MP-AVT-215.

Hitzel, S. M., Boelens, O. J., van Rooij, M. and Hövelmanm, A. (2016) 'Vortex Development on the AVT-183 Diamond Wing Configuration – Numerical and Experimental Findings', *Aerospace Science and Technology*, 57, 90 – 102. https://doi.org/10.1016/j.ast.2015.12.007

Hitzel, S., Winkler, A. and Hövelmann, A. (2020) *Vortex Flow Aerodynamic Challenges in the Design Space for Future Fighter Aircraft,* in Dillmann A. et al. (Eds.) *New Results in Numerical and Experimental Fluid Mechanics XII.* Springer Nature : Switzerland, 142, pp. 297–306. https://doi.org/10.1007/978-3-030-25253-3_29. Retrieved from www.scopus.com

Holdaway, G. H. and Mellenthin, J. A. (1960). Investigation at Mach Numbers of 0.20 to 3.5 of Blended wing body combinations of Sonic Design with Diamond, Delta and Arrow Plan forms. NASA Technical Memorandum X-372.

Hövelmann, A. and Breitsamter C. (2012) Aerodynamic Characteristic of the Sagitta Diamond Wing Demonstrator Configuration. In *61st Deutscher Luft- und Raumfahrtkongress*. 10 – 12 September. Berlin, Germany: ID: 281220.

Hövelmann, A. and Breitsamter, C. (2013) Leading- Edge Geometry Effects on the Vortex System Formation of a Diamond Wing Configuration. In *31st AIAA Applied Aerodynamics Conference*. 24 – 27 June. San Diego, United States: AIAA 2013-3187.

Hövelmanm, A. and Breitsamter, C. (2014) Experimental Investigations on Vortex Flow Phenomena of a Diamond Wing Configuration. In *29th Congress of the International Council of the Aeronautical Sciences*. 7-12 September. St. Petersburg, Russia: ICAS2014_0024.

Hövelmann, A., Grawunder, M., Buzica, A., and Breitsamter, C. (2016) 'Diamond Wing Flow Field Characteristics Part 2: Experimental Analyses on Leading-edge Vortex Formation and Progression', *Aerospace Science and Technology,* 57, 31–42.

Hövelmann, A., Knoth, F., and Breitsamter, C. (2016) 'AVT-183 Diamond Wing Flow Field Characteristics Part 1: Varying Leading-edge Roughness and The Effects on Flow Separation Onset', *Aerospace Science and Technology,* 57, 18 – 30.

Htun, Y. E., Yar, Z. A. Y., and Myint, M. Y. O., (2016) 'Some principles of flow visualisation techniques in wind tunnel', *International Journal of Advances in Science Engineering and Technology*, 4(2), 62 – 66.

Hummel, D. (1979). On the vortex formation over a slender wing at large incidence. AGARD-CP-247, Paper No. 15.

Hummel, D. (2004) *Effects of Boundary layer Formation on the vortical Flow above Slender Delta Wings*. RTO specialist Meeting on Enhancement of NATO military Flight Vehicle Performance by Management of Interacting Boundary Layer transition and Separation. Meeting Proceedings RTO-MPAVT- 111, pp. 30-1 – 30-2.

Hummel, D. (2008) Chapter *35 – Final Results of the International Vortex Flow Experiments –Résumé and Outlook*. RTO-TR-AVT-113.

Hummel, D. (2013) 'The International Vortex Flow Experiment 2 (VFE-2): Background, Objectives and Organization', *Aerospace Science and Technology*, 24(1), pp. 1 - 9.

Hummel, D., and Cummings, R. M. (2013). Special Issue, VFE-2. *Aerospace Science and Technology,* 24(1).

Jiang, F., Lee, G. B., Tai, Y. C. and Ho, C. M. (2000) 'A flexible Micromachinebased Shear Stress sensor array and its application to separation point detection', *Sensors and Actuators,* 79, pp.194-203.

Jirasek, A., Cummings, R. M., Schütte, A., and Huber, K. (2014) The NATO STO AVT-201 Task Group on Extended Assessment of Stability and Control Prediction Methods for NATO Air Vehicles: Summary. In *32nd AIAA Applied Aerodynamics Conference.* 16 – 20 June. Atlanta, Georgia: AIAA 2014-2394.

Jones, R., Miles, J. W. and Pusey, J. S. (1954) *Eksperiments in the Compressed Air Tunnel on Swept-back Wings Including Two Delta Wings*. London, British Aeronautical Council Report and Memoranda: R.&M. No. 2871.

Kasim, K. A. (2017) Propeller Locations Study on Delta Winged Unmanned Aerial Vehicle (UAV) Model. Master Thesis, Universiti Teknologi Malaysia, Skudai.

Kaushik, M. (2019) *Finite Wing Theory*. In *Theoretical and Experimental Aerodynamics*. Singapore: Springer. doi: 10.1007/978-981-13-1678-4_6.

Konrath, R., Klein, C., Engler, R.H. and Otter, D. (2006). Analysis of PSP Results Obtained for the VFE-2 65^0 Delta Wing Configuration at Sub- and Transonic

Speeds. In *24th Applied Aerodynamics Conference*. 5 - 8 June. San Francisco, California : AIAA 2006-3003.

Konrath, R., Klein, C. and Schröder, A. (2013) 'PSP and PIV Investigation on the VFE-2 Configuration in Sub- and Transonic Flow', *Aerospace Science and Technology*, 24(1), 22 - 31.

Kulfan, R. M. (1979). Wing Geometry Effects on Leading Edge Vortices. In *Aircraft Systems and Technology Meeting*. 20 – 22 August. New York : 79-1872.

Kulite Semiconductor Product, Inc. *Kulite XCL-072 Miniature Transducer Manual*. New Jersey, 2009.

Lang, N. (1998). PIV Measurements in Sub- and Supersonic Flow over the Delta Wing Configuration ELAC. In *8th International Symposium on Flow Visualization*. 1- 4 September. Sorrento, Italy.

Lamar, J. E. and Hummel, D. (2008) *Chapter 1 – RTO Task Group AVT-113 Understanding and Modelling Vortical Flows to Improve the Technology Readiness Level for Military Aircraft: Objectives and Overview*. RTO-TR AVT-113.

Lambourne, N. and Bryer, D. W. (1961) *The Bursting of Leading-edge Vortices: Some Obervations and Discussion of Phenomenon*. Aeronautical Research Council. Reports and Memoranda: No. 3282.

Luckring, J. M. (2004) Reynolds Number, Compressibility, and Leading Edge Bluntness Effects on Delta Wing Aerodynamics. In *24th International Congress of the Aeronautical Sciences*. 29 – 3 September. Yokohama, Japan: ICAS 04-414.

Luckring, J. M. (2008) *Chapter 18 – Initial Experimental and Analysis of Blunt-Edge Vortex Flows*. RTO-TR-AVT-113.

Luckring, J. M. (2010) A Survey of Factors Affecting Blunt Leading-Edge Separation for Swept and Semi-Slender Wings. In *28th AIAA Applied Aerodynamics Conference*. 28 June - 01 July. Chicago, United States: AIAA 2010-4820.

Luckring, J. M. (2013) 'Initial Experiments and Analysis of Blunt-edge Vortex Flows for VFE-2 configurations at NASA Langley, USA', *Aerospace Science and Technology,* 24(1), 10 - 21.

Luckring, J. M. (2019) 'The discovery and prediction of vortex flow aerodynamics', *The Aeronautical Journal*, 123(1264), 729-804.

Luckring, J. M. and Boelens, O. J. (2011) *A Unit-Problem Investigation of Blunt Leading-Edge Separation Motivated by AVT-161 SACCON Research*. RTO-MP-AVT-189.

Luckring, J. M. and Hummel, D. (2013) 'What Was Learned From The New VFE-2 Experiments', *Aerospace Science and Technology,* 24(1), 77- 88.

Luckring, J. M., Boelens, O. J., Breitsamter, C., Hövelmann, A., Knoth, F., Malloy, D. J. and Decke, S. (2016) 'Objectives, approach, and scope for the AVT-183 diamond-wing investigations', *Aerospace Science and Technology*, 57, 2 – 17.

Manshadi, M. D., Mehdi Eilbeigi, M., Sobhani, M. K., Zadeh, M. B. and Vaziry, M. A. (2016) 'Experimental study of flow field distribution over a generic cranked double delta wing', *Chinese Journal of Aeronautics*, 29(5), 1196-1204.

Maqsood, A. and Go, T. H. (2015) 'Aerodynamic characteristics of a flexible membrane micro air vehicle', *Aircraft Engineering and Aerospace Technology*, 87(1), pp. 30-37.

Mat, S. B., (2011). *The analysis of flow on round-edged delta wings.* PhD Thesis, University Of Glasgow, United Kingdom.

Mat, S., Ishak, I. S., Lazim, T.M., Mansor, S., Said, M., Rahman, A.B.A, Kamaludim, A.S.A., Brossay, R. (2014) 'Development of Delta Wing Aerodynamics Research in Universiti Teknologi Malaysia Low Speed Wind Tunnel', *Journal of Advances in Mechanical Enigeering,* 2014, pp. 434892 – 434902.

Mat. S., Green, R., Galbraith, R. and Coton, F. (2015) 'The Effect of Edge Profile on Delta Wing Flow', *Proceedings of the Institution of Mechanical Engineers, Part G: Journal of Aerospace Engineering,* 230(7), pp. 1252-1262.

Miller, D. S. and Wood, R. M. (1985). *Lee-Side flow over delta wings at supersonic speeds.* NASA TP 2430.

Mitchell, A. M. (2003) Experimental Data Base Selected for RTO/AVT Numerical and Analytical Validation and Verification: ONERA 70-Deg Delta Wing. In *21st AIAA Applied Aerodynamics Conference, Fluid Dynamics and Co-located Conferences*. 23 - 26 June. Orlando, Florida : AIAA 2003-3941.

Noor, A. M. and Mansor, S. (2013) 'Measuring Aerodynamic Characterisitcs Using High Performance Low Speed Tunnel at University Teknologi Malaysia', Journal of Applied Mechanical Engineering, 2(5), pp. 1-7.

Oberkampf, W. L. and Trucano, T. G. (2002) 'Verification and validation in computational fluid dynamics', *Progress in Aerospace Science*, 38, 209-272.

Osterhuber, R. (2013) FCS-requirements for Combat Aircraft – Lessons Learned for Future Designs. In *STO AVT Workshop on Innovative Control Effectors for Military Vehicles*. 20 – 22 May. Stockholm, Sweden: No. KN-5, STO-MP-AVT-215.

Peake, D. J. and Tobak, M. (1980). *Three-Dimensional Interactions and Vortical Flows with Emphasis on High Speeds*. AGARD-AG-252.

Peckham, D. H. and Atkinson, S. A. (1960). *Preliminary Results of Low Speed Wind Tunnel Tests on a Gothic Wing of Aspect Ratio 1.0*. Aeronautical Research Council Technical Report : R21836.

Peng, S. H. (2016) Verification of RANS and Hybrid RANS-LES Modelling in Computations of a Delta-Wing Flow. In *46th AIAA Fluid Dynamics Conference*. 13-17 June. Washington, D.C.: AIAA 2016-3480.

Pershing, B. (1964). *Separated Flow Past Slender Delta Wings Wit Secondary Vortex Simulation*. El Segundo Techical Operations. TDR–269(4560 – 10) – 4.

Pevitt, C., and Alam, F. (2014) 'Static Computational Fluid Dynamics simulations around a specialised delta wing', *Computers & Fluids,* 100, 155-164.

Pfnür, S. and Breitsamter, C. (2018) 'Unsteady aerodynamics of a diamond wing configuration', *CEAS Aeronautical Journal*, 9, pp. 93–112. https://doi.org/10.1007/s13272-018-0280-9

Polhamus, E. C. (1966). A Concept of the vortex Lift of Sharp-Edged Delta Wings Based on a Leading-Edge Suction Analogy. NASA TN-D-3767.

Rein, M. and Gardne, A. D. (2015) 'Generic Lambda Wing Configuration in Compressible Flow: Effect of Highly Integrated Intakes', *Journal of Aircraft*, 52(3), 972 – 980.

Renac, F., Barberis, D. and Molton, P. (2005) 'Control of Vortical Flow over a Rounded Leading- Edge Delta Wing', *AIAA Journal*, 43(7), 1409-1417.

Riley, A. J. and Lowson, M. V. (1998) 'Development of a three-dimensional free shear layer', *Journal of Fluid Mechanics*, 369, 49-89.

Rinoie, K. (1996) *Low Speed Aerodynamics Characteristics of 60^0 Rounded Leading-Edge Delta Wing with Vortex Flaps: Part 1: 457 mm Span Delta Wing*. Cranfield University. COA Report No. 9611.

Riou, J., Garnier, E. and Basdevant, C. (2010) 'Compressibility Effects on the Vertical Flow over a 65° Sweep Delta Wing', *Physic of Fluids*. 22, 035102.

Rogalski, T., Rzucidło, P. and Prusik, J. (2020) 'Unmanned aircraft automatic flight control algorithm in a spin maneuver', *Aircraft Engineering and Aerospace Technology*, 92(8), 1215-1224.

Said, M., Mat, S., Mansor, S., Abdul-Latif, A., and Lazim, T. M. (2015). Reynolds Number Effects on Flow Topology Above Blunt-Edge Delta Wing VFE-2 Configuration. In *53rd AIAA Aerospace Sciences Meeting*. 5 – 9 January. Kissimmee, Florida: AIAA 2015-1229.

Said, M. (2016) *Effects of Leading Edge Radius, Reynold Number and Angle of Attack on the Vortex Formation above Large-edged Delta Wing*. Master Thesis, Universiti Teknologi Malaysia, Skudai.

Schiavetta, L. A., Boelens, O. J., Crippa, S., Cummings, R. M., Fritz, W., and Badcock, K. L. (2009) 'Shock Effects on Delta Wing Vortex Breakdown', *AIAA Journal of Aircraft*, 46(3), 903-914.

Schütte, A. (2016) Numerical investigations of the vortical flow on swept wings with round leading edges. In *34th AIAA Applied Aerodynamics Conference.* 13-17 June. Washinton, D.C. : AIAA 2016-4172.

Schütte, A., Vormweg, J., Maye, R. G. and Jeans, T. L. (2018) Aerodynamic shaping design and vortical flow design aspects of a 53deg swept flying wing configuration. In *2018 Applied Aerodynamics Conference*. 25-29 June. Atlanta, Georgia : AIAA 2018-2841.

Sepulveda, E. and Smith, H. (2017) 'Technology challenges of stealth unmanned combat aerial vehicles', *Aeronautical Journal,* 121(1243), 1261-1295.

Sepulveda, E., Smith, H. and Sziroczak, D. (2019) Multidisciplinary analysis of subsonic stealth unmanned combat aerial vehicles. *CEAS Aeronautical Journal.* 10, 431–442.

Shabudin Mat (2010) *The Analysis of Flow on Round-Edged Delta Wings*. PhD Thesis, University of Glasgow, United Kingdom.

Tajuddin, N. (2021) *Vortices Characterization on Blunt-Edged VFE-2 Delta Wing at Subsonic Flow Regime*. Master Thesis, Universiti Teknologi Malaysia, Skudai.

Taylor, G. S., Schnorbus, T. and Gursul, I. (2003) An investigation of vortex flows over low sweep delta wings. In *33rd AIAA Fluid Dynamics Conference and Exhibit*. 23-26 June. Orlando, Florida : AIAA-2003-4021.

Wang, J. and Tu, J. (2010) ‘Effect of wing planform on leading-edge vortex structures’, *Chinese Science Bulletin*, 55, pp. 120–123. doi: 10.1007/s11434-009-0643-z.

Wang, J. J. and Zhan, J. X. (2005) ‘New Pair of Leading-Edge Vortex Structure for Flow over Delta Wing’, *Journal of Aircraft*, 42(3), pp. 718-721. doi: 10.2514/1.9929.

Wang, J. J. and Zhang, W. (2008) 'Experimental Investigations on Leading-Edge Vortex Structures for Flow over Non-Slender Delta Wings', *Chinese Physics Letters*, 25(7), 2550-2553.

Wang, J. J., Zhao, X., Liu, W. C. , and Tu, J. Q. (2007) 'Experimental investigation on flow structures over nonslender delta wings at low Reynolds numbers', *Journal of Experiments in Fluid Mechanics*, 21, 1–7.

Yaniktepe, B., and Rockwell, D. (2004) ‘Flow Structure on a Delta Wing of Low Sweep Angle’, *AIAA Journal,* 42(3), pp. 513-523.